Published in final edited form as:
Cancer Res. 2008 December 15; 68(24): 10247–10256. doi:10.1158/0008-5472.CAN-08-1494.

Systemic Blockade of Transforming Growth Factor-β (TGF-β) Signaling Augments the Efficacy of Immunogene Therapy

Samuel Kim[1], **George Buchlis**[1], **Zvi G. Fridlender**[1], **Jing Sun**[1], **Veena Kapoor**[1], **Guanjun Cheng**[1], **Andrew Haas**[1], **Hung Kam Cheung**[2], **Xiamei Zhang**[2], **Michael Corbley**[2], **Larry R. Kaiser**[1], **Leona Ling**[2], and **Steven M. Albelda**[1]

1*Thoracic Oncology Research Laboratory, 1016B ARC, University of Pennsylvania, 3615 Civic Center Blvd., Philadelphia, PA 19104-6160*

2*Oncology Cell Signaling, Biogen Idec, 12 Cambridge Center, Cambridge, MA 02142*

Abstract

Locally-produced TGF-β promotes tumor-induced immunosuppression and contributes to resistance to immunotherapy. This paper explores the potential for increased efficacy when combining immunotherapies with TGF-β suppression using the TGF-β type I receptor kinase inhibitor, SM16. Adenovirus expressing IFNβ (Ad.IFNβ) was injected intratumorally once in established subcutaneous AB12 (mesothelioma) and LKR (lung cancer) tumors or intratracheally in a K-ras orthotopic lung tumor model. Mice bearing TC1 (lung cancer) tumors were vaccinated with two injections of adenovirus expressing HPV-E7 (Ad.E7). SM16 was administered orally in formulated chow. Tumor growth was assessed and cytokine-expression and cell populations were measured in tumors and spleens by real time-PCR and flow cytometry. SM16 potentiated the efficacy of both immunotherapies in each of the models and caused changes in the tumor microenvironment. The combination of SM16 and Ad.INFβ increased the number of intratumoral leukocytes (including macrophages, NK cells, and $CD8^+$ cells) and increased the percentage of T-cells expressing the activation marker CD25. SM16 also augmented the anti-tumor effects of Ad.E7 in the TC1 flank tumor model. The combination did not increase HPV-E7 tetramer-positive $CD8^+$ T cells in the spleens, but did induce a marked increase in the tumors. Tumors from SM16-treated mice showed increased mRNA and protein for immunostimulatory cytokines and chemokines, as well as endothelial adhesion molecules, suggesting a mechanism for the increased intratumoral leukocyte trafficking. Blockade of the TGF-β signaling pathway augments the anti-tumor effects of Ad.INFβ immune-activating or Ad.E7 vaccination therapy. The addition of TGF-β blocking agents in clinical trials of immunotherapies may increase efficacy.

Keywords

tumor immunology; immunosuppression; TGFβ; tumor associated macrophages; cytokines; lung cancer; mesothelioma; tumor vaccine; interferon-β

Introduction

It has become increasingly apparent that cancer cells alter their adjacent microenvironment to form a permissive and supportive environment for tumor progression (1–6). Tumor-induced immunosuppression is one of the most important of these adaptations and inhibits endogenous

Requests for reprints: Steven Albelda, Thoracic Oncology Research Laboratory, 1016B ARC, University of Pennsylvania, 3615 Civic Center Blvd., Philadelphia, PA 19104-6160, Phone, 215-573-9933; Fax, 215-573-4469; E-mail: E-mail: albelda@mail.med.upenn.edu.

anti-tumor immune responses, as well as presenting a formidable block against any immunotherapy approaches used to treat the tumor (7,8).

Current immunotherapies (such as immuno-gene therapy with cytokines, tumor vaccines, and adoptive T cell transfer) are primarily aimed at initiating or boosting the immune response to tumors and their antigens. However, the effectiveness of these therapies may be limited by the local immunosuppressive environment of the tumor. In particular, the immunosuppressive cytokine, TGF-β, is overexpressed by tumors. Evidence suggests TGF-β production by tumors plays a significant role in blocking immune response (9). Specifically, recent findings implicate this multifunctional cytokine in preventing T cell infiltration into tumors, inhibition of T cell activation/function, and mediation of T regulatory cell-induced immunosuppression (10–14). For example, evidence links clinical resistance to tumor vaccine therapy in glioblastoma patients to TGFβ expression levels (15).

TGF-β's pivotal role in suppressing the anti-tumor immune response has made it a logical target for the development of antagonists to block its biological effects (9). We and others have shown that TGF–β blockers (soluble receptors/antibodies) and TGF–β receptor inhibitors have anti-tumor effects that, in several models, are due primarily to immunologic mechanisms (16–19). For example, we found that TGF-β blockade had anti-tumor effects in a murine malignant mesothelioma model and that this activity was $CD8^+$ T-cell dependent (18,19). In these models, TGF-β blockade resulted in the persistence of tumor-killing $CD8^+$ T-cells harvested from the spleens of the tumor-bearing animals and increased numbers of $CD8^+$ T-cells within tumors of animals treated with a soluble TGF-β receptor (18). Similar findings were observed when we used SM16, a small, orally available type I TGF–β receptor (Alk-5/Alk4) kinase inhibitor that can effectively block SMAD phosphorylation within tumors (19). In our studies, and in those of Ge et al. (16) and Nam et al. (17), anti-tumor effects were markedly reduced in immunodeficient animals.

Given this augmentation of endogenous anti-tumor immunity, we hypothesized that combining systemic TGF-β receptor blockade with active immunotherapy would result in enhanced responses compared to either approach alone. To test this hypothesis, we combined SM16 with two immunogene therapy approaches that we characterized previously: 1) delivery of the cytokine, interferon-β, using an adenoviral vector (Ad.IFNβ) (20,21), and 2) vaccination using an adenoviral vector expressing a known tumor antigen (Human papilloma virus-E7 protein [HPV-E7]) (22). In each case, we found marked augmentation of efficacy using combined therapy, along with evidence of increased leukocyte infiltration, including intratumoral $CD8^+$ T cells that were antigen-specific or showed increased expression of the activation marker CD25.

Materials and Methods

Animals

Mice were purchased from Taconic Labs (Germantown, NY) or Jackson Labs (Bar Harbor,ME). Breeding pairs of Lox-Stop-Lox (LSL) KrasG12D mice (on mixed 129Sv.J and C57BL/6 background) used in the orthotopic lung model were initially provided by Dr. David Tuveson (21). The Animal Use Committee of the University of Pennsylvania approved all protocols in compliance with the Guide for the Care and Use of Laboratory Animals.

Cell lines

A murine malignant mesothelioma cell line, AB12, derived from an asbestos-induced tumor in a Balb/C mouse, has been previously described in detail (19,20,23). The murine lung cancer line "LKR" was derived from an explant of a pulmonary tumor from an activated Kras G12D

mutant mouse that had been induced in an F1 hybrid of 129Sv.J and C57BL/6 (21). TC1 cells were derived from mouse lung epithelial cells derived from a C57B6 mouse and immortalized with HPV-16 E6 and E7 and transformed with the c-Ha-ras oncogene (24). All cell lines were injected into the appropriate syngeneic strain.

SM16, a TGFβ Receptor Kinase Inhibitor

The chemical structure of SM16, a 430MW ALK4/ALK5 kinase inhibitor produced by BiogenIdec has recently been published (25). This small molecule can be administered as formulated in mouse chow which allows for daily oral administration (19). We have previously shown that SM16 chow at a dose of 0.45 g/kg of chow is well tolerated by the animals, results in therapeutic drug levels, and effectively blocks SMAD2 phosphorylation within tumor cells (19).

TGFβRII/Fc protein

A soluble recombinant murine TGF-β receptor type II-murine Fc: IgG2a chimeric protein has been described previously (18). It binds and inhibits TGF-β1 and -β3 in the 1 nM range and has a half-life in mouse plasma of 14 days. Previous studies have shown biological effects at 1 mg/kg, 2 mg/kg, and 5 mg/kg.

Animal Flank Tumor Models

Mice were injected on the right flank with 1×10^6 AB12, LKR, and TC1 tumor cells in the appropriate syngeneic host. The flank tumors were allowed to reach an average size of 200–250 mm^3 (approximately 14–17 days). Following treatments as outlined below, tumor growth was followed with measurement twice weekly. All experiments had at least 5 mice per group and were repeated at least once.

Treatment with oral SM16 chow and intratumoral Ad-INF β combination

The effect of combining oral SM16 with intratumoral Ad.INF-β therapy (10^9 pfu of virus) was studied by treating tumor-bearing mice (AB12 and LKR). Mouse chow formulated with SM16 (0.45g/kg chow) was given ad libitum starting when the flank tumors reached average size of 200–250 mm^3 (approximately 14– 17 days). One dose of 1×10^9 pfu of Ad.INFβ was injected intratumorally 6–7 days after SM16 treatment. The mice were followed closely and tumors were measured twice weekly.

Treatment with oral SM16 chow and/or intra-tracheal Ad-INF β therapy in orthotopic lung cancer model

The orthotopic lung cancer model using intra-tracheal Ad-INFβ therapy has been previously described in detail (21). Briefly, to induce tumors, 100 μl of saline containing 3×10^{10} particles of adenovirus containing Cre recombinase (Ad.Cre) was administered to all LSL KrasG12D mice intranasally. Four groups of mice (n=8 per group) were studied. One group got no further treatment. One group received only SM16-formulated chow starting 18 days post Ad.Cre treatment. One group received one dose of 1×10^9 pfu Ad-INFβ intra-tracheally on Day 21. The final group (Combo group) got both SM16-formulated chow starting 18 days post Ad.Cre treatment and received one dose of 1×10^9 pfu Ad-INFβ intra-tracheally on Day 21. When animals appeared lethargic, had ruffled fur, or increased breathing rate, they were sacrificed.

Oral SM16 treatment with Ad.E7 vaccination in the TC1 tumor model

An E1/E3-deleted Type 5 adenoviral vector expressing the HPV-E7 protein under control of a cytomegavirus promoter (Ad.E7) has been previously described (22). To test the effects of combination treatment, animals bearing TC1 tumors (approximately 200mm^3 in size) were

vaccinated s.c in the left flank (contralateral to the tumor) with 1×10^9 plaque forming units (pfu) of Ad.E7 vector. The next day, oral chow formulated with SM16 (0.45mg/kg chow) was started. Seven days following the initial vaccination, mice received a booster vaccine of 1×10^9 pfu of Ad.E7 in the left flank. Control animals received regular chow.

TGFβRII/Fc protein with Ad.E7 vaccination in the TC1 model

To test the effects of combination treatment using a different type of TGF-β inhibitor with the Ad.E7 vaccine, animals bearing large TC1 tumors (approximately 500 mm^3 in size) were left untreated or vaccinated s.c in the left flank (contralateral to the tumor) with 1×10^9 plaque forming units (pfu) of Ad.E7 vector. Five days later, i.p. injections of the TGFβRII/Fc protein (1 mg/kg every three days for three doses) were started in one group of control and one group of vaccinated animals. The next day (seven days following the initial vaccination), vaccinated mice received a booster vaccine of 1×10^9 pfu of Ad.E7 in the left flank. Each group had 5 mice.

Flow Cytometric Analysis of Tumors and spleen after SM16 and AdE7 vaccination treatment

In the Ad.INF-β models, FACS on tumors was performed two days after the dose of Ad.IFN-β. In the vaccination model, spleens were harvested for FACS seven days after the second Ad.E7 vaccination (previously determined to be the time of optimal response) and tumors were harvested for FACS two days after the second Ad.E7 vaccination (a time when the tumor size was similar among groups). Splenocytes and tumor cells were studied by FACS analysis as previously described (22). The APC-labeled H-$2D^b$ tetramer (1:200 dilution) loaded with E7 peptide (RAHYNIVTF) was obtained from the NIAID tetramer core. The fluorescently labeled antibodies were all purchased from BD Bioscience. Glow cytometry was done using a Becton Dickinson FACS Calibur flow cytometer (San Jose, CA). Data analysis was done using FlowJo software (Ashland, OR).

RNA isolation and real time, reverse transcription-PCR

To evaluate changes in the tumor microenvironment induced by SM16, mice with tumors (approximately 200 mm^3) were treated with SM16 chow or control chow (n=5 in each group). Tumors were removed after 5 days, flash frozen, and the RNA from each tumor isolated. For both treatment conditions, a pool of RNA was created by adding the same amount of RNA from each of the five tumors within the group. cDNA was made from each pool, RNA levels were normalized to β-actin levels and quantification of tumor mRNA levels was performed as previously described (26). Relative levels of expression of each of the selected gene (fold change in SM16-treated versus control) were determined. Each sample was run in quadruplicate and the experiment was repeated at least once.

Intratumoral Cytokine Assays

Mice were treated as above. Tumors were removed at 5 days after treatment, sonicated for 30 seconds, spun at 3000 RPM for 10 minutes and filtered through a 1.2 micron syringe filter unit. Total protein in each individual sample (n= 5 in each group) was determined. Mouse cytokine expression for each sample was measured using a multiplex Luminex® bead assay system as previously described (26).

Statistical Analyses

For the RT-PCR and protein experiments comparing differences between two groups, we used unpaired Student t-tests. For FACS studies and flank tumor studies comparing more than two groups, we used ANOVA with appropriate post hoc testing. For the modified survival study (Fig. 1D), we used Kaplan-Meier survival curves and analyzed with the Mantel-Cox log rank

test. Differences were considered significant when P<0.05. Data are presented as mean+/− SEM.

RESULTS

SM16 Augments Immunotherapies in Multiple Tumor Models

The effect of simultaneous TGF-β receptor blockade and immune activation was examined by combining SM16 treatment with two immuno-gene therapy models.

First, the combination of SM16 with Ad-INF-β was tested in two independent tumor models known to respond to Ad-IFN-β (20,21). Mice bearing large AB12 (malignant mesothelioma) or LKR (lung cancer) flank tumors (approximately 200–250 mm^3), began daily oral administration of SM16 or were given control chow. Seven days later, one dose of Ad-INF-β was administered intra-tumorally. As shown in Figure 1A, treatment of AB12 tumors with either SM16 alone or Ad.INF–β was only minimally effective in inhibiting the growth of these large tumors. In contrast, treatment with the combination of SM16 and Ad.IFN-β, resulted in marked shrinkage of the tumors, with tumors being significantly smaller ($p<0.05$) than that of control or single treatments at all time points measured. Impressively, combination therapy led to complete tumor regression in 3 of 5 animals versus no complete regressions in any other group. In the LKR model (Fig 1B), Ad.INF-β alone temporarily slowed the growth of large tumors, whereas SM16 treatment actually decreased the size of the tumors and induced one complete regression. However, combination therapy was even more effective ($p<0.05$ compared to control and each treatment alone), rapidly shrinking all tumors and eventually inducing complete remissions in 4 of the 5 tumors.

We also performed a modified survival study using mice that conditionally express an oncogenic KrasG12D allele. LSL-KrasG12D positive mice were intratracheally injected with Ad.Cre. Eighteen days later (at a time of detectable tumor burden (21)), mice were started on either SM16-containing chow or regular chow. Three days later (Day 21), one dose of 1×10^9 of Ad.INF-β was administered intra-tracheally. As shown in Figure 1C, the median survival time for control mice was 46 days, with all mice sacrificed by 52 days. SM16-treated mice and Ad.INF-β-treated mice had small, but significantly prolonged median survivals ($p<0.05$) compared to the control, but there was no difference between the SM16 treatment and Ad.INF-β treatment groups. However, in the group that received both SM16 and Ad.INF-β treatment, median survival was doubled compared to control (82 days). This increase was significant compared to all the other groups ($p<0.01$).

Next, we examined whether TGFβ receptor blockade potentiated a tumor antigen vaccine approach (Fig. 2A). As previously observed (22), treatment of established TC1 tumors with two doses of Ad.E7 alone, led to significant ($p<0.05$) slowing of tumor growth compared with control, but did not induce tumor regression. Treatment with oral SM16 led to a similar, significant ($p<0.05$) degree of tumor slowing. There were no significant differences in tumor size between SM16 and Ad.E7 groups. In contrast, treatment with the combination of Ad.E7 and SM16 led to clear tumor regression. The tumors in the combination group were statistically smaller than control tumors ($p<0.01$) and tumors from the SM16 alone and Ad.E7 alone treatment groups ($p<0.05$). An independent replicate of this study is shown in Supplemental Figure 1.

To confirm that this augmentation was not due to an “off–target” effect of the TGF-β receptor blocker, we conducted a similar study (in very large TC1 tumors) using Ad.E7 in combination with sTGFβRII:Fc, a soluble TGFβ receptor fusion protein that binds TGF-β1 and TGF-β3, functioning like a neutralizing antibody (18). As shown in Figure 2B, the size of tumors in the combination group were significantly smaller than those in the single treatment groups.

SM16 Alters the Tumor Microenvironment by Increasing Immunostimulatory Cytokines and ICAM-1

To assess the effect of SM16 alone on the tumor microenvironment, the effects of five days of SM16 treatment on a variety of cytokine and chemokine mRNA levels within the tumors was measured by quantitative PCR. As shown in Table 1A, SM16 induced significant increases in the messenger RNA levels of a number of inflammatory cytokines and chemokines including TNFα, INF-γ, IL-1β, IL-6, IP10 (CXCL10), MIG (CXCL9), and MCP-1 (CCL2). Significant changes were also seen in message levels of key enzymes that affect arginine metabolism (which affects T-cell activation): arginase was down-regulated and iNOS was upregulated.

Although protein measurements of tissue cytokines are subject to a number of limitations (such as uncontrolled proteolysis and variation in efficiency of protein extraction), we also made homogenates of AB12 tumors and analyzed them using a Luminex Bead assay. As shown in Table 1B, values measured from the SM16-treated versus control tumors, showed significant increases in a number of cytokines and chemokines including RANTES, MCP-1, MIP1α, and IL-6, although there was not perfect correspondence with the RT-PCR data.

In addition, the message level of the cell adhesion molecule, ICAM-1, increased by 1.5–2.6 fold. To determine if this increase reflected augmented protein expression on tumor endothelial cells, FACS analysis was performed on pooled samples of tumors in which intratumoral endothelial cells (EC) were identified as the $CD45^{-}/CD31^{+}$ cells. As shown in Figure 3A, the mean fluorescent intensity (MFI) of ICAM-1 on EC from control tumors versus SM16 treated tumors increased from 69.5 versus 108.9 on AB12 tumors, 34.2 versus 66.0 in LKR tumors, and 24.8 to 50.2 on TC1 tumors. These studies were repeated in an independent experiment with very similar results.

SM16 Increases the Percentage and the Functional Status of $CD8^{+}$ cells in Tumors from All Three Models

To assess the effect of SM16 on the presence of $CD8^{+}$ T cells and other leukocytes in tumors, mice were treated for one week with SM16 or control chow, tumors were harvested and subjected to FACS. This time point was chosen because after one week of treatment, the tumors have responded to SM16, but are still large enough for analysis. Figure 4 and Supplemental Table 1 summarizes this data.

In all three cell lines, treatment with SM16 (compare “control” with “SM16” in each panel of Figure 4) resulted in significant ($p<0.05$) increases in the percentage of total cells in the tumor of $CD45^{+}$ cells and $CD8^{+}$ cells. In AB12 and LKR cells, significant ($p<0.05$) increases in $CD11b^{+}$ cells were also seen. In AB12 cells, the number of NK cells increased significantly ($p<0.05$).

To assess the activation state of these cells, we also used FACS to investigate the expression of CD25 (a T cell activation marker (27,28)) in $CD8^{+}$ T cells from AB12 or LKR tumors treated with SM16 versus control. Representative examples for AB12 tumors using dot plots are shown in Figure 3B. Data from all 5 tumors in each group was compared using the mean fluorescence intensity of CD25 on $CD8^{+}$ T cells. In control-treated AB12 tumors MFI was 4.0 +/−0.5. However, SM16-treated tumors showed a significant 2-fold increase in CD25 expression compared to control tumors (MFI of 7.9 +/−0.8, $P<0.05$). In LKR tumors, expression of CD25 was higher on the $CD8^{+}$ T-cells at baseline (MFI 15.2 +/− 0.4), but again, SM16 treatment significantly increased expression of CD25 (MFI of 25.8+/− 4.1, $p<0.05$).

Combination of SM16 with Immunotherapies Significantly Increases Tumor-Associated CD8$^+$ Cells and Myeloid Cells More Than Single Agent Therapy

We next tested the hypothesis that changes in tumor-associated immune cells correlated with the enhanced efficacy seen with the combination treatments in Figure 1 and Figure 2. The leukocyte cell populations were thus measured as a percentage of total cells from tumors using FACS, two days after Ad.IFN-β in the AB12 or LKR models (which was 1 week following initiation of SM16 therapy in the SM16 alone or combination treatment regimens) or two days after the second dose of Ad.E7 in the TC1 model. At this time point, the tumors were large enough for analysis, but showed regression in response to combination therapy or evidence of growth inhibition with single agent treatment (Figure 4 and Supplemental Table 1).

Figure 4 (with details in supplemental Table 1) illustrates that in all three models tested, the percentages of CD45$^+$, CD11b$^+$, CD8$^+$, and NK$^+$ cells were generally significantly increased ($p< 0.05$) in the tumors treated with combination therapy when compared to untreated tumors or the tumors treated with single therapies. The most dramatic changes were seen in the vaccine model, where the combination of SM16 and Ad.E7 markedly increased three populations of tumor-associated immune cells. The overall leukocyte population in the combination group constituted 57 percent of all tumor cells with 16.8% of tumor cells represented by CD8$^+$ cells and 21% of tumor cells by CD11b$^+$ cells. These percentages were, respectively, 5.7-fold, 56-fold and 2-fold higher than in the tumors from vehicle-treated mice. In all three models, CD4$^+$ cells were present only as a very low percentage of total tumor cells ((<0.7%) and were not significantly changed by the treatments. The percentage of CD25-expressing CD4$^+$ T cells was not increased with combination treatment compared to SM16 treatment (Supplemental Table 1).

Antigen Specific T Cells in the Ad.E7 Model

The TC1/Ad.E7 model provided the opportunity to measure the effects of each treatment on T cells directed at the immunodominant tumor antigen using MHC Class I tetramers loaded with the appropriate HPV-E7 peptide.

As shown in Figure 5A (averages of five mice per group) and Figure 5B (representative examples), in control, tumor-bearing animals, an average of 1.4% of the CD8$^+$ cells in the spleen were tetramer positive. This represents a relatively weak endogenous anti-tumor response. Treatment with SM16 alone did not significantly increase this percentage (1.7%). As we have previously reported (22), Ad.E7 vaccination significantly ($p<0.05$) increased the percentage of tetramer-positive CD8$^+$ T cells to 5.3% (a 3.8 fold increase compared to control). The tetramer-positive percentage in the Combination group (6.3%) was significantly ($p<0.05$) increased (4.5 fold) compared to the control and SM16 group, but was not statistically different from the Ad.E7 alone treatment group. Thus, neither SM16, nor the combination treatment, caused a systemic enhancement in anti-tumor T cells greater than Ad.E7 alone.

Figure 5C (also see Supplemental Table 1 and Figure 4F), shows that the percentage of CD8$^+$ cells within individual tumors was markedly increased by combination therapy. After a Ficoll gradient spin, CD8$^+$ cells from individual tumors were pooled and analyzed for expression of the tetramer. As shown in Figure 5D, the percentage of intratumoral CD8$^+$ T cells that were tetramer-positive at baseline and after SM16 treatment alone was approximately 10%. As might be expected, Ad.E7 therapy increased this percentage to 16.9%. However, in the combination group, the percentage of tetramer positive cells rose significantly, to more than 50%. Thus, in this model, the combination of SM16 and Ad.E7 appears to markedly increase the localization of anti-tumor CD8$^+$ T cells to the tumor microenvironment, rather than enhance the systemic population of tumor-directed CD8$^+$ T cells.

Discussion

The studies presented here using the ALK5/AlK4 inhibitor, SM16, in three different syngeneic tumor models (AB12 mesothelioma, LKR and TC-1 lung carcinomas), in flank and orthotopic models, and with two different immune-activating therapies (Ad.E7 and Ad.INF-β) support the utility of combining inhibition of TGF-β signaling with immune-activating therapies. These results show that TGF-β receptor blockade via SM16 can augment a variety of adenovirus-based, immune-activating therapies in a spectrum of tumors. Similar results using a soluble TGF-β receptor (Fig. 2B) suggest that our findings are applicable to other TGF-β blocking strategies.

Analysis of the mechanism of action in each model highlight the similarities and differences between the response of these tumor models to these therapies. A common finding was an increase in intratumoral $CD8^+$ T cells, that was augmented significantly in the combination treatments (Fig. 4). This effect is consistent with the previously described mechanisms of action for SM16, Ad.INF-β and Ad.E7 (18–20). However, the increase in tumor-associated NK ($NK1^+$) and macrophages ($CD11b^+$) cells with SM16 alone, in both the AB12 and LKR models, identifies a novel response to TGF-β inhibition. Interestingly, tumor-associated $CD11b^+$ cells were not increased by SM16 in the TC-1 model, suggesting inherently different immunosuppressive mechanisms may be in play in these different models. However, a further enhancement of $CD11b^+$ and $NK1^+$ populations by the combination treatments above the single agent treatments was a common feature in all three tumor models. These data support the utility of the combination treatments in models where different immunosuppressive mechanisms may be operative.

Another novel finding was the ability of TGF-β receptor blockade alone to cause significant alterations in the tumor microenvironment favoring T cell activation and the Th1 phenotype, as well as T cell and leukocyte infiltration. SM16 treatment induced the expression of the message levels for cytokines which are chemoattractive for T cells and NK cells (29). An increase in tumor endothelial ICAM-1 expression and the enhanced expression of message levels for TNFα, INF-γ and IL-1β, cytokines which stimulate adhesion molecule expression, are also consistent with a process that would increase T cell and leukocyte infiltration (30). It should be noted that our RT-PCR results did not show perfect correlation with intra-tumoral cytokine measurements, however, this could be due to difficulties in sample proteolysis and inefficient extraction from tumor specimens.

The SM16-induced increase in the percentage of activated $CD8^+$ T cells ($CD25^+$), the increased Th1 cytokines, and the decreased arginase message levels also suggest that TGF-β blockade promotes a tumor environment promoting the activation of tumor-associated T cells. This is consistent with previous reports showing TGF-β induces macrophage arginase levels (31) and is inhibitory to T cell activity via inhibition of INF-γ and perforins (12,13). In the TC-1 model, Ad.E7 treatment alone increased tetramer-positive T cells in both the spleen and tumors, while SM16 had no effect on this T cell population in either location on its own. However, the combination of SM16 and Ad.E7 induced a further increase in tumor-associated, tetramer-positive cell above that induced by Ad.E7, with no significant change in splenic tetramer-positive cells. These results suggest that TGF-β receptor blockade does not increase the overall number of tetramer-positive T cells, but does increase either the trafficking or persistence in the tumor of this anti-tumor T cell population. These findings suggest that TGF–β is a key, proximal immunosuppressive modulator of the tumor microenvironment that can inhibit T cell and leukocyte trafficking, function, or persistence in tumors.

We have emphasized the role of TGF-β on immune cells, however, interpretation of our studies needs to take into account the complexity of the role of TGF-β in tumor biology (1,2,8) since

multiple cells within a tumor make, activate, and respond to TGF-β. For example, using genetic models of mammary carcinogenesis in mice that result in selective loss of TGF-β signaling in tumor cells, investigators have observed marked changes in the secretion of specific chemokines by tumor cells that appear to then alter the tumor-associated myeloid cell populations and the tumor microenvironment (32,33). As another example, loss of TGF-β receptor expression in lung cancer cells has been associated with increased invasiveness and increased production of the chemokine CCL5 (34). Our experiments use a "global" inhibitor that would presumably block TGF-β signaling in stromal cells, leukocytes, and in the tumor cells themselves (cell autonomous effects). It is currently unclear, how important the blockade of each cell type might be. Additional effects of TGF-β on tumor biology could also be involved in anti-tumor effects, such as a recent report suggesting that TGF-β could subvert the immune system in directly promoting tumor growth through interleukin-17 (35).

One issue that should be considered with any type of inhibitor compound is that of specificity. As recently published (25), the activity of SM16 (similar to other such inhibitors like SD-093 or SD208 (16)) is primarily directed against ALK5 (Ki: 10 nM) and ALK4 (Ki: 1.5 nM), although there is some moderate off-target activity to Raf (IC_{50} 1 uM) and p38/SAPKa (IC_{50}, 0.8 uM). To try to address the question of off-target effects, we performed a study with the Ad.E7 vaccine in combination with a completely different class of TGF-β blocking agent, a soluble Type I receptor (18), and showed very similar effects as we saw with SM16 (Fig. 2B).

Previous studies have shown increased immunogenicity and anti-tumor responses when TGF-β inhibition (mediated by antisense oligonucleotides or dominant negative receptors) is targeted to tumor cells and immune cell types, which are then used as vaccines or in adoptive transfer (36–40). Some of these approaches are moving into clinical trials (41–44). There are only a limited number of reports where systemic inhibitors of TGF-β have been combined with immunotherapy in the intact animal, however. Some success in a rat model of glioma has been achieved by combining intracranial injection of anti-sense TGF-β2 oligonucleotides with an irradiated tumor cell line (plus interferon-γ) (45). Induction of anti-TGF-β antibodies by injection of plasmid DNA encoding a xenopus TGF-β5 gene increased the therapeutic efficacy of a tyrosinase-related protein-2 plasmid DNA vaccine (46). Perhaps most relevant to this study, is a report by Kobie et al. (47) showing that administration of an antibody against TGF-β enhanced the ability of an intratumorally injected DC vaccine to inhibit the growth of established mouse breast cancer cells.

These aforementioned studies, as well as others, have revealed the immunosuppressive effects of TGF-β in blocking systemic generation or function of anti-tumor T cells (16,17) and mediating T regulatory cell activity (48). However, the experiments presented here identify additional mechanisms directed at immune and inflammatory cell infiltration, function, or persistence that may play an important role when combining TGF-β inhibition with immune-promoting therapies. These local intratumoral effects of TGF-β blockade may be extremely important, since many cancer patients progress despite exhibiting relatively high percentages of circulating anti-tumor T-cells (i.e., in melanoma) or showing the presence of T cells surrounding tumor tissue (49), supporting the idea that T-cells must be able to move into the tumor, survive there, and effectively exert their direct and indirect (macrophage and NK cell activation) anti-tumor activities to be effective (50). Consistent with this idea, we have recently shown that after adoptive T-cell transfer, the number of cytotoxic T cells with tumors is enhanced after blockade of TGF-β receptor function (51).

Individual immune-activating therapies, such as tumor and dendritic cell vaccines, adoptive immune cell transfer, and adenovirus-based therapies (including Ad.INF-β), are now being tested as single agents in clinical trials (52–54). The work presented here, and that of others in

the field, suggest that a greater potential for efficacy may be achieved by combining these therapies with treatments targeting key modulators of immunosuppression, such as TGF-β, in order to promote an “immune-friendly” tumor microenvironment.

Supplementary Material

Refer to Web version on PubMed Central for supplementary material.

Abbreviations

Ad, adenovirus
EC, endothelial cells
GM-CSF, granulocyte-macrophage colony stimulating factor
HPV-7, human papilloma virus E7 protein
ICAM-1, intercellular adhesion molecule-1
iNOS, inducible nitric oxide synthetase
IFNβ, interferon β
IFNγ, interferon γ
IL, interleukin
IP10, interferon-inducible protein-10
MIP-1α, macrophage inflammatory protein–1α
MCP-1, monocyte chemotactic protein-1
MIG, monokine induced by γ-interferon
MFI, mean fluorescent intensity
pfu, plaque forming units
RANTES, Regulated on Activation Normal T-cell Expressed Secreted
TNFα, tumor necrosis factor-α
Tregs, Tregulatory cells

Acknowledgements

The authors thank Drs. Anil Vachani, Daniel Heitjan, and Leslie Litzky for their assistance. This work was funded by NCI PO1 CA 66726 and P30 ES013508-02 from the National Institute of Environmental Health Sciences (NIEHS), NIH. Its contents are solely the responsibility of the authors and do not necessarily represent the official views of the NIEHS, NIH.

Grant support:

NCI PO1 CA 66726

References

1. Mueller MM, Fusenig NE. Friends or foes - bipolar effects of the tumour stroma in cancer. Nat Rev Cancer 2004;4:839–849. [PubMed: 15516957]
2. Bhowmick NA, Moses HL. Tumor-stroma interactions. Curr Opin Genet Dev 2005;15:97–101. [PubMed: 15661539]
3. Kim R, Emi M, Tanabe K, Arihiro K. Tumor-driven evolution of immunosuppressive networks during malignant progression. Cancer Res 2006;66:5527–5536. [PubMed: 16740684]
4. Gajewski TF, Meng Y, Harlin H. Immune suppression in the tumor microenvironment. J Immunother 2006;29:233–240. [PubMed: 16699366]
5. Rodriguez PC, Ochoa AC. T cell dysfunction in cancer: Role of myeloid cells and tumor cells regulating amino acid availability and oxidative stress. Seminars in Cancer Biology 2006;16:66–72. [PubMed: 16298138]
6. Rabinovich GA, Gabrilovich D, Sotomayer EM. Immunosuppressive strategies that are mediated by tumor cells. Annu Rev Immunol 2007;25:267–296. [PubMed: 17134371]

7. Lizee G, Radvanyi LG, Overwijk WW, Hwu P. Improving antitumor immune responses by circumventing immunoregulatory cells and mechanisms. Clin Cancer Res 2006;12:4794–4803. [PubMed: 16914564]
8. Whiteside TL. Immune suppression in cancer: Effects on immune cells, mechanisms and future therapeutic intervention. Seminars in Cancer Biology 2006;16:3–15. [PubMed: 16153857]
9. Elliott RL, Blobe GC. Role of transforming growth factor beta in human cancer. J Clin Oncol 2005;23:2078–2093. [PubMed: 15774796]
10. Gorelik L, Flavell RA. Transforming growth factor-beta in T-cell biology. Nat Rev Immunol 2002;2:46–53. [PubMed: 11905837]
11. Li MO, Wan YY, Sanjabi S, Robertson AK, Flavell RA. Transforming growth factor-beta regulation of immune responses. Annu Rev Immunol 2006;24:99–146. [PubMed: 16551245]
12. Ahmadzadeh M, Rosenberg SA. TGF-beta 1 attenuates the acquisition and expression of effector function by tumor antigen-specific human memory CD8 T cells. J Immunol 2005;174:5215–5223. [PubMed: 15843517]
13. Thomas DA, Massague J. TGF-β directly targets cytotoxic T cell functions during tumor evasion of immune surveillance. Cancer Cell 2005;8:369–380. [PubMed: 16286245]
14. Marie JC, Letterio JJ, Gavin M, Rudensky AY. TGF-β1 maintains suppressor function and Foxp3 expression in $CD4^+CD25^+$ regulatory T cells. J Exp Med 2005;201:1061–1067. [PubMed: 15809351]
15. Liau LM, Prns RM, Liertscher SM, et al. Dendritic cell vaccination in glioblastoma patients induces systemic and intracranial T-cell responses modulated by the local central nervous system tumor microenvironment. Clin Can Res 2005;11:5515–5525.
16. Ge R, Rajeev V, Ray P, et al. Inhibition of growth and metastasis of mouse mammary carcinoma by selective inhibitor of transforming growth factor-β type I receptor kinase in vivo. Clin Cancer Res 2006;12:4315–4330. [PubMed: 16857807]
17. Nam J-S, Terabe M, Mamura M, et al. An anti-transforming growth factor β antibody suppresses metastasis via cooperative effects on multiple cell compartments. Cancer Res 2008;68:3835–3843. [PubMed: 18483268]
18. Suzuki E, Kapoor V, Cheung HK, et al. Soluble type II Transforming Growth Factor-β Receptor inhibits both small and large established murine malignant mesothelioma tumor growth by augmenting host anti-tumor immunity. Clin Can Res 2004;10:5907–5918.
19. Suzuki E, Kim S, Cheung HK, Corbley M, et al. A Novel Small Molecule Inhibitor of TGF-beta type I Receptor Kinase (SM16) Inhibits Murine Mesothelioma Tumor Growth *in vivo* and Prevents the Extent of Tumor Recurrence After Surgical Resection. Cancer Res 2007;67:2351–2359. [PubMed: 17332368]
20. Odaka M, Sterman D, Wiewrodt R, Zhang Y, Kiefer M, Amin K, Gao G-P, Wilson JM, Barsoum J, Kaiser LR, Albelda SM. Eradication of intraperitoneal and distant tumor by adenovirus-mediated interferon-beta gene therapy due to induction of systemic immunity. Cancer Research 2001;61:6201–6212. [PubMed: 11507073]
21. Wilderman M, Sun J, Khan M, Vachani A, et al. Intrapulmonary interferon-beta gene therapy using an adenoviral vector is highly effective in a murine orthotopic model of lung adenocarcinoma via a combination of direct toxicity, NK cell, and CD8 T-cell mediated effects. Cancer Res 2005;65:8379–8387. [PubMed: 16166316]
22. Haas A, Sun J, Vachani A, Wallace AF, Silverberg M, Kapoor V, Albelda SM. Cyclooxygenase-2 Inhibition augments efficacy of a cancer vaccine. Clinical Cancer Research 2006;12:214–222. [PubMed: 16397045]2006
23. Davis MR, Manning LS, Whataker D, Garlepp MJ, Robinson BWS. Establishment of of a murine model of malignant mesotheoioma. Int. J. Cancer 1992;52:881–886. [PubMed: 1459729]1992
24. Lin KY, Guarnieri FG, Staveley-O'Carroll KF, et al. Treatment of established tumors with a novel vaccine that enhances major histocompatibility class II presentation of tumor antigens. Cancer Res 1996;56:21–26. [PubMed: 8548765]
25. Fu K, Corbley MJ, Sun L, et al. An Orally Active Inhibitor of the TGF-β Type I Receptor, ALK5, Inhibits Vascular Fibrosis and Adventitial Myofibroblast Induction in the Rat Carotid Balloon Injury Model. Arteriosclerosis, Thrombosis, Vascular Biology 2008;28:665–671.

26. Jassar A, Suzuki E, Kapoor V, et al. Activated tumor-associated macrophages and $CD8^+$ T-cells are the key mediators of anti-tumor effects of the vascular disrupting agent 5,6 Di-methylxanthenone-4-acetic Acid (DMXAA) in murine models of lung cancer and mesothelioma". Cancer Res 2005;65:11752–11761. [PubMed: 16357188]2005
27. Quezada SA, Peggs KS, Curran MA, Allison JP. CTLA4 blockade and GM-CSF combination immunotherapy alters the intratumor balance of effector and regulatory T cells. J Clin Invest 2006;116:1935–1945. [PubMed: 16778987]
28. Serafini P, Meckel K, Kelso M, et al. Phosphodiesterase-5 inhibition augments endogenous antitumor immunity by reducing myeloid-derived suppressor cell function. J Exp Med 2006;203:2691–2702. [PubMed: 17101732]
29. Vicari AP, Caux C. Chemokines in cancer. Cytokine Growth Factor Rev 2002;13:143–154. [PubMed: 11900990]
30. Carlos TM. Leukocyte recruitment at sites of tumor: dissonant orchestration. J Leukoc Biol 2001;70:171–184. [PubMed: 11493608]
31. Boutard V, Havouis R, Fouqueray B, Philippe C, Moulinoux JP, Baud L. Transforming growth factor-beta stimulates arginase activity in macrophages. Implications for the regulation of macrophage cytotoxicity. J Immunol 1995;155:2077–2084. [PubMed: 7636258]
32. Bierie B, Stover DG, Abel TW, et al. Transforming growth factor-beta regulates mammary carcinoma cell survival and interaction with adjacent microenvironment. Ca Res 2008;68:1809–1819.
33. Yang L, Humang J, Ren X, et al. Abrogation of TGFβ signaling in mammary carcinomas recruits GR-1+CD11b+ myeloid cells that promote metastatsis. Cancer Cell 2008;13:23–35. [PubMed: 18167337]
34. Borczuk AC, Papanikolaou N, Toonkel , et al. Lung adenocarcinoma invasion in TGFβRII-deficient cells is mediated by CCL5/RANTES. Oncogene 2007;27:557–564. [PubMed: 17653092]
35. Nam J-S, Terabe M, Kang M-J, et al. Transforming growth factor-beta subverts the immune system into directly promoting tumor growth through interleukin-17. Ca Res 2008;68:3915–3923.
36. Wang FL, Qin WJ, Wen WH, Tian F, et al. TGF-β insensitive dendritic cells: an efficient vaccine for murine prostate cells. Cancer Immunol Immunother 2007;56:1785–1793. [PubMed: 17473921]
37. Gorelik L, Flavell RA. Immune-mediated eradication of tumors through the blockade of transforming growth factor-β signaling in T cells. Nature Med 2001;7:1118–1122. [PubMed: 11590434]
38. Bollard C, Rossig C, Calonge MJ, Huls MH, et al. Adapting a transforming growth factor-β-related tumor protection strategy to enhance antitumor immunity. Blood 2002;99:3179–3187. [PubMed: 11964281]
39. Lucas P, McNeil N, Hilgenfeld E, Choudhury B, et al. Transforming growth factor-β pathway serves as a primary tumor suppressor in $CD8^+$ T cell tumorigenesis. Cancer Res 2004;64:6524–6529. [PubMed: 15374963]
40. Zhang Q, Yang X, Pins M, Javonovic B, et al. Adoptive transfer of tumor-reactive transforming growth factor-β-insenstive CD8+ T cells: Eradication of autologous mouse prostate cancer. Cancer Res 2005;65:1761–1769. [PubMed: 15753372]
41. Nemunaitis J, Dillman RO, Scharzenberger PO, Senzer N, et al. Phase II study of belagenpmatucel-L, a transforming growth factor beta-2 antisense gene-modified allogeneic tumor cell vaccine in non-small-cell lung cancer. J Clin Oncol 2006;24:4271-30.
42. Arteaga C. Inhibition of TGFβ signaling in cancer therapy. Cur Opin in Genetics and Develop 2006;16:30–37.
43. Yingling JM, Blanchard KL, Sawyer JS. Development of TGF-β signaling inhibitors for cancer therapy. Nat Rev 2004;3:1011–1022.
44. Iyer S, Wang ZG, Akhtari M, Zhao W, Seth P. Targeting TGFβ signaling for cancer therapy. Cancer Biol and Therapy 2005;4:261–266.
45. Liu Y, Want Q, Kleinschmidt-DeMasters BK, Franzusoff A, et al. TGF-B2 inhibiton augments the effect of tumor vaccine and improves the survival of animals with pre-established brain tumors. J Neurooncol 2007;81:149–162. [PubMed: 16941073]
46. Jia ZC, Zou LY, Ni B, Wan Y, et al. Effective induction of antitumor immunity by immunization with plasmid DNA encoding TRP-2 plus neutralization of TGF-β. Cancer Immunol Immunother 2005;54:446–452. [PubMed: 15750831]

47. Kobie JJ, Wu RS, Kurt RA, et al. Transforming growth factor beta inhibits the antigen-presenting functions and antitumor activity of dendritic cell vaccines. Cancer Res 2003;63:1860–1864. [PubMed: 12702574]

48. Yu P, Lee Y, Liu W, Krausz T, et al. Intratumor depletion of $CD4^+$ cells unmasks tumor immunogenicity leading to the rejection of late-stage tumors. J Exp Med 2005;201:779–791. [PubMed: 15753211]

49. Rosenberg SA, Sherry RM, Morton KE, et al. Tumor progression can occur despite the induction of very high levels of self/tumor antigen-specific CD8+ T cells in patients with melanoma. J Immunol 2005;175:6169–6176. [PubMed: 16237114]

50. Frey AB, Monu N. Effector-phase tolerance: another mechanism of how cancer escapes antitumor immune response. J Leukoc Biol 2006;79:652–662. [PubMed: 16415165]

51. Wallace A, Kapoor V, Sun J, Mrass P, Weninger W, Heitjan DF, June C, Kaiser L, Ling LE, Albelda SM. TGF-β receptor blockade augments the effectiveness of adoptive T-cell therapy of established solid tumors. Clin. Cancer Res 2008;14:3966–3974. [PubMed: 18559619]

52. Berzofsky JA, Terabe M, Oh S, Belyakov IM, et al. Progress on new vaccine strategies for the immunotherapy and prevention of cancer. J Clin Invest 2004;113:1515–1525. [PubMed: 15173875]

53. Rosenberg SA, Yang JC, Restifo NP. Cancer immunotherapy: moving beyond current vaccines. Nat Med 2004;9:909–915. [PubMed: 15340416]

54. Sterman DH, Recio AR, Carroll RG, Gillespie C, et al. A Phase I Clinical Trial of Single-Dose Intrapleural Interferon-Beta Gene Transfer For Malignant Mesothelioma and Metastatic Pleural Effusions: High Rate of Anti-Tumor Immune Responses. Clin Ca Res 2007;13:4456–4466.

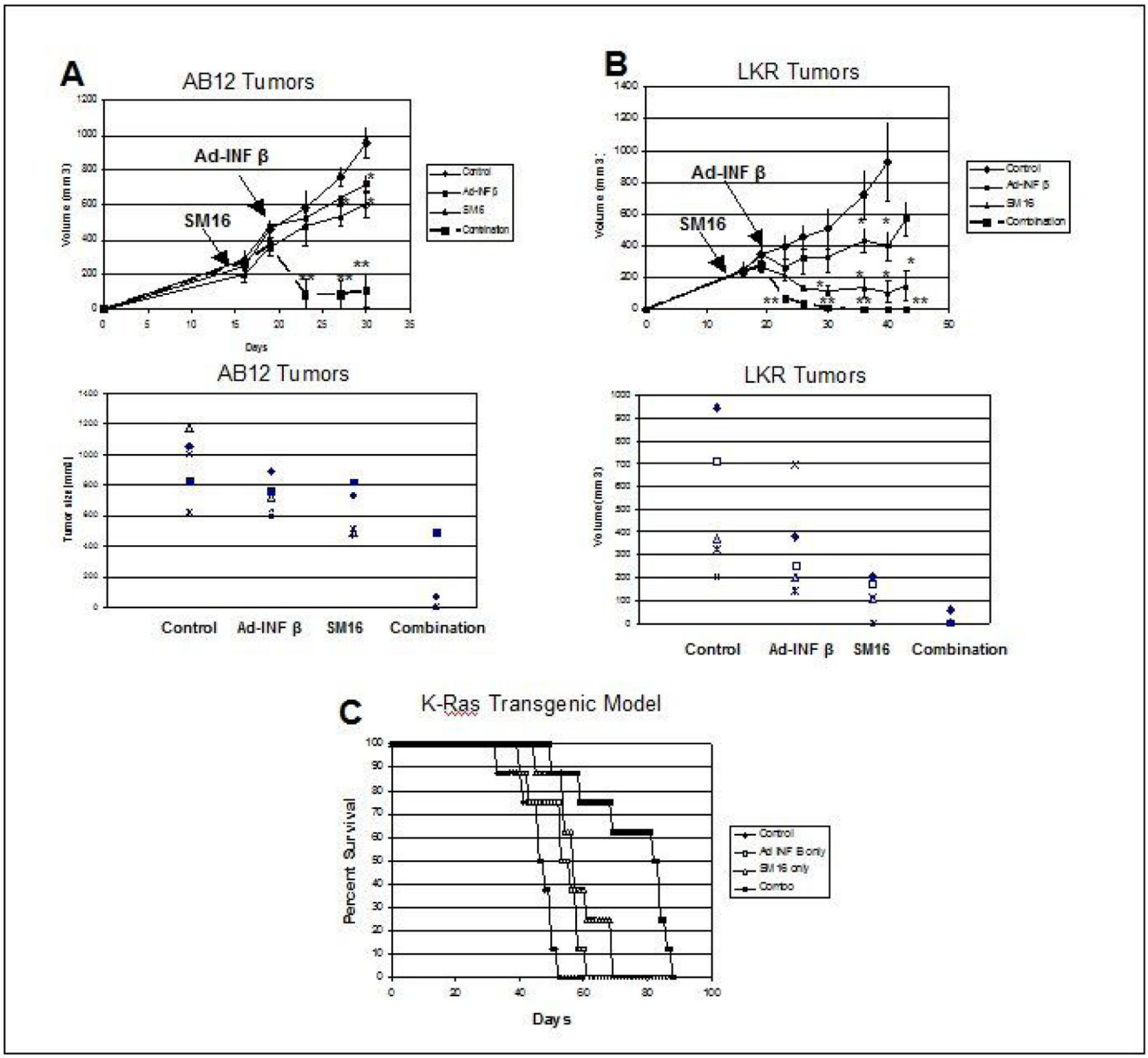

Figure 1. Effect of SM16 on Ad.IFN-β Immuno-gene Therapy Models

Panels A and B. Mice (n = 5 for each group) bearing large tumors (approximately 200–250 mm^3), were treated in one of four ways: 1) one group was left untreated (diamonds-control); 2) one group (SM16) was placed on the TGF-β receptor kinase inhibitor chow for the duration of the experiment (see arrows)(triangles-SM16); 3) one group (small squares-Ad-INFβ) was injected with one dose of Ad.INFβ (1×10^9 pfu) 7 days later (see arrow) and 4) one group (large squares- Combo) received Ad.INFβ plus SM16 chow (see arrows). Tumor volumes were measured every three days.

Panel A shows results in the AB12 mesothelioma model. The top graph shows growth curves and the bottom graph shows the tumor sizes in each animal at time of sacrifice on Day 30. ** = $p<0.05$ compared to all other groups. * = $p<0.05$ compared to control.

Panel B shows results in the LKR lung cancer model. The top graph shows growth curves and the bottom graph shows the tumor sizes in each animal at time of sacrifice on Day 40. ** = $p<0.05$ compared to all other groups. * = $p<0.05$ compared to control.

Panel C. LSL-KrasG12D positive mice (that conditionally express an oncogenic KrasG12D allele) were intratracheally injected with Ad.Cre on Day 0 (to activate the "floxed" mutated Kras transgene). Eighteen days later, treatment groups (n=8) were established: Control (diamonds) got no other treatment; SM16 group (triangles) were started on SM16-containing chow; Ad.INFβ group (open squares) got one dose of 1×10^9 pfu of Ad.INFβ intratracheally on Day 21; Combination group (filled squares) got the SM16 diet and one dose of Ad.INFβ. Mice were followed until they started to show signs of distress and were then sacrificed. SM16-treated mice and Ad.INF-β-treated mice had small, but significantly prolonged median survivals ($p<0.05$) compared to the control. There was no significant difference in "survival" times between the SM16 treatment and Ad.INF-β treatment group. However, in the group that received both SM16 and Ad.INF-β treatment, median survival was significantly increased compared to all the other groups ($p<0.01$).

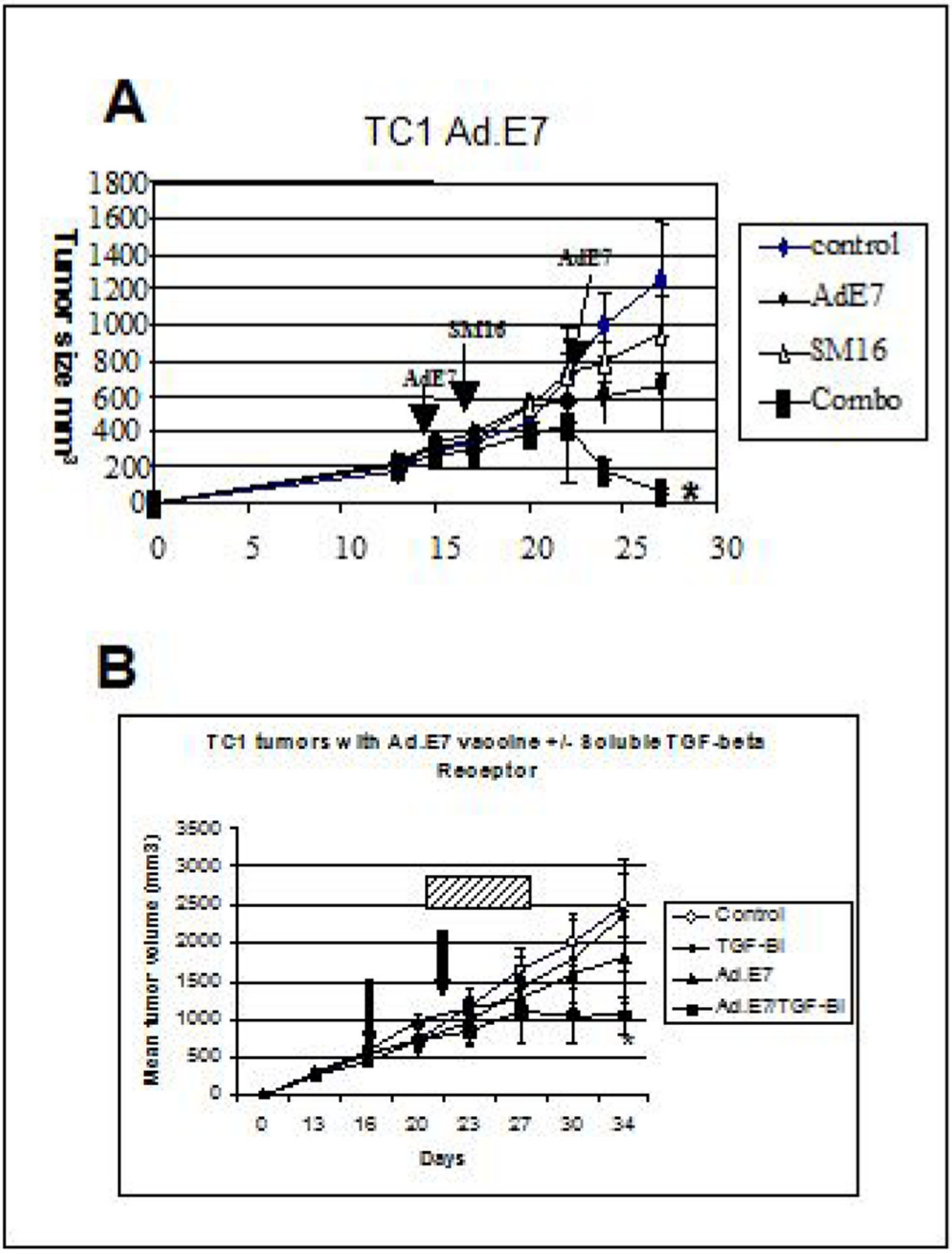

Figure 2. Effect of SM16 on Ad.E7 Immuno-gene Vaccine Model

Panel A. Mice (n=5 for each group) bearing large TC1 tumors (approximately 200mm^3), were treated in one of four ways: 1) one group was left untreated (diamonds-control); 2) one group (SM16) was placed on the TGF-β receptor kinase inhibitor chow for the duration of the experiment (see arrows)(triangles- SM16) ; 3) one group (Ad.E7) was injected with 2 ×10^9 pfu of Ad.E7 subcutaneously in the contralateral flank, with a second dose given 7 days later (see arrows) (circles- AdE7) and 4) one group (Combo) received the two doses Ad.E7 plus SM16 chow (beginning the day after the first dose of Ad.E7) (see arrows) (squares). Tumor volumes were measured every three days. The tumors from mice in the Combo group were statistically

smaller than control tumors ($p<0.01$) and tumors from the SM16 alone and Ad.E7 alone treatment groups ($p<0.05$) (*).

Panel B. Mice were treated as above, except instead of using SM16 chow, TGF-β was blocked using intraperitoneal injections of 1 mg/kg TGFβRII/Fc protein every three days for 3 doses (hatched bar). The tumors from mice in the Combo group were statistically smaller than control tumors and tumors from the TGF-β inhibitor and Ad.E7 alone treatment groups ($p<0.05$) (*).

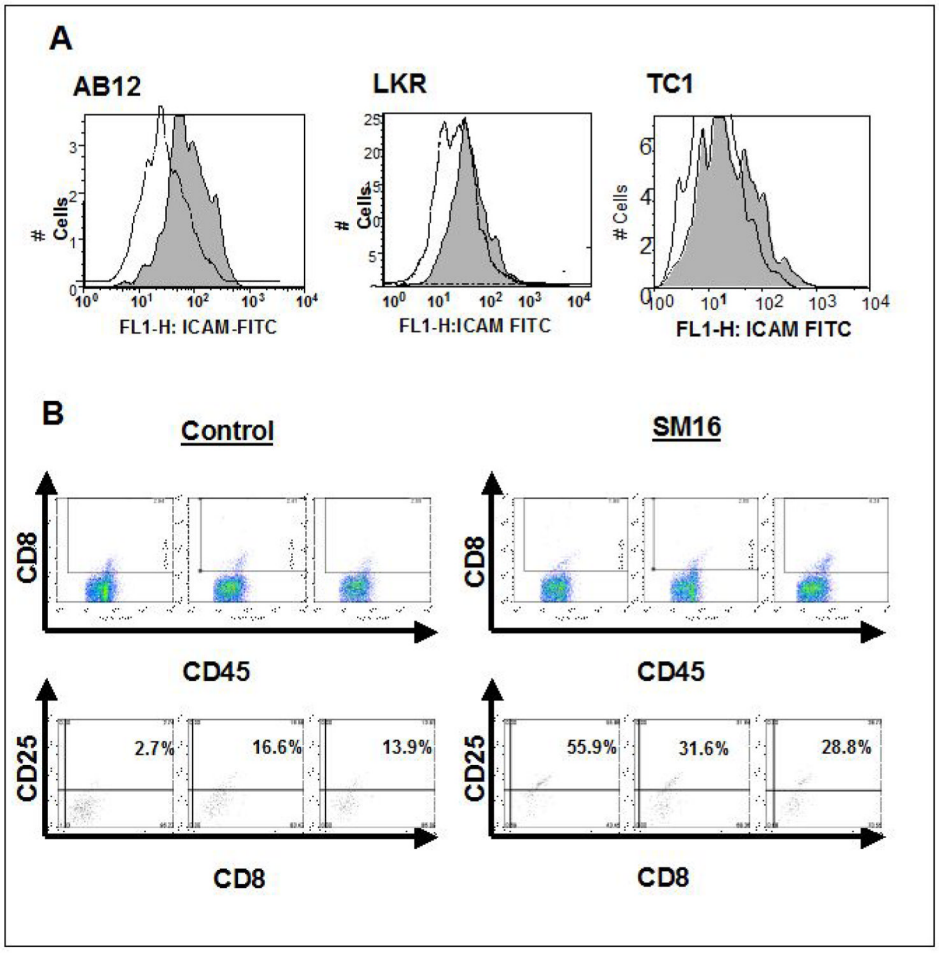

Figure 3. FACS Analysis of Tumor Cells

Panel A. Three-color flow cytometry was performed on digested tumors from animals treated with control chow (dotted line-white shading) or SM16 chow (solid line-gray shading). Histograms of the ICAM-1 expression of the $CD45^{-}/CD31^{+}$ cell population (endothelial cells) is shown.

Left graph: AB12 tumors (MFI control: 69.5; MFI SM16-treated: 108.9)

Middle graph: LKR tumors (MFI control: 34.2; MFI SM16-treated: 66)

Right: TC1 tumors (MFI control: 24.8; MFI SM16-treated: 50.2)

Panel B. The activation state of the $CD8^{+}$ T cells obtained from three AB12 tumors from control animals and from three AB12 tumors from animals treated for one week with SM16 was determined by FACS staining for the activation marker CD25. The detection gates were set using an isotype control antibody that included less than 1% of cells. The upper panels show the population of $CD8^{+}/CD45^{+}$ cells (boxed area) identified from each tumor. In the lower panel, the expression of the activation marker CD25 was determined from these $CD8^{+}$ cells. The number in each box, represents the percentage of CD8 cells expressing CD25 above the threshold gate. The percentage of positive cells was significantly greater ($p<0.05$) in the SM16 versus control groups.

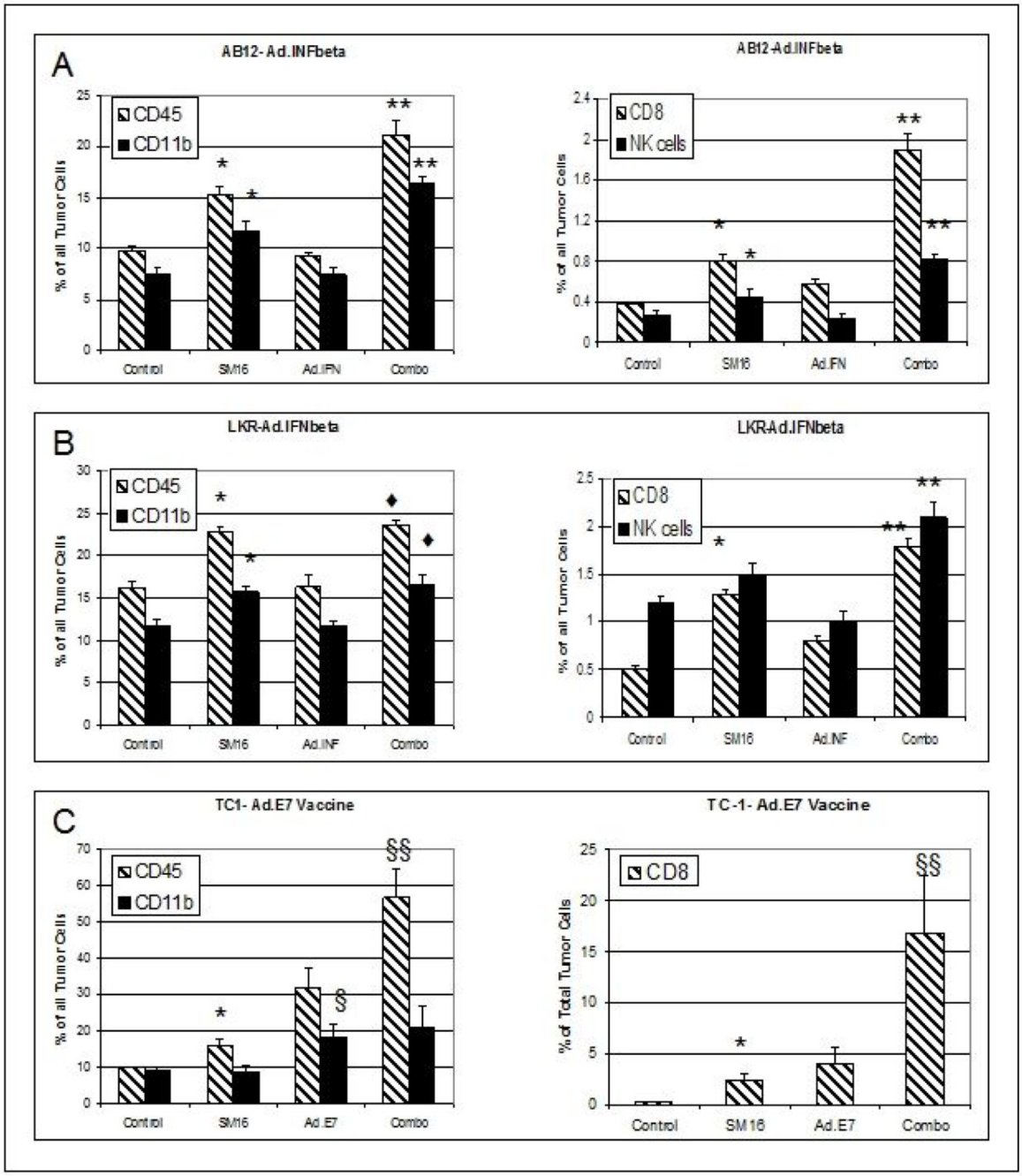

Figure 4. FACS Analysis of Leukocytes within Treated Tumors

Panels A–B. Mice (n=5 per group) were treated with control chow, SM16, one dose of Ad.IFNβ, or the combination (combo) of SM16 and Ad.IFNβ. AB12 tumors (Panel A) or LKR tumors (Panel B) were removed from all groups two days after Ad.IFN-β had been administered (i.e. Day 22 in Figure 1), digested, and subjected to FACS. The data are presented as mean +/− SEM for each group. The left graphs show the percentage of $CD45^+$ cells and $CD11b^+$ cells of total tumor cells. The right graphs show the percentage of $CD8^+$ T cells and $NK1.1^+$ cells of total tumor cells.

* = $p<0.05$ between control vs SM16 group

** = $p<0.05$ between combo group vs control, SM16, and Ad.IFNβ groups.

♦= $p<0.05$ between combo group vs control and Ad.IFNβ groups

Panels C. TC1 tumor-bearing mice were treated with control chow, SM16, two doses of Ad.E7 or the combination (combo) of SM16 and Ad.E7. Tumors were removed from all groups two days after Ad.E7 had been administered (i.e. Day 24 in Figure 2A), digested, and subjected to FACS. The left graph shows the percentage of $CD45^+$ cells and $CD11b^+$ cells of total tumor cells. The right graph shows the percentage of $CD8^+$ T cells of total tumor cells.

* = $p<0.05$ between control vs SM16 group

§ = $p<0.05$ between combination vs control, SM16, an Ad.E7

§§ = $p<0.05$ between combination vs control and SM16

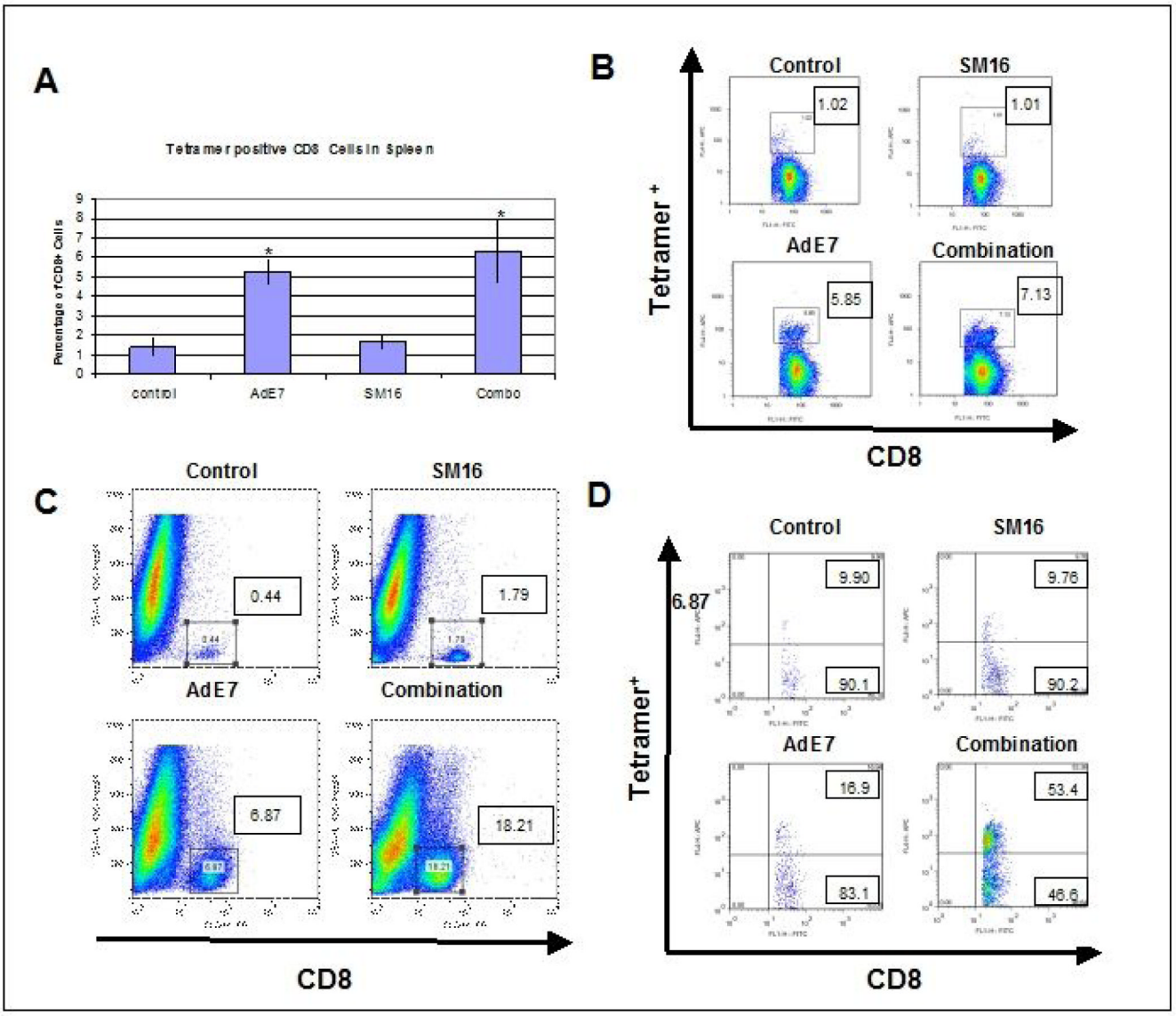

Figure 5. FACS Analysis of Leukocyte Populations in Spleens and Tumors in the Ad.E7/TC1 Vaccine Model

Panels A and B: Tetramer staining of splenocytes. Spleens of animals from each group (n=5) (control, Ad.E7, SM16, and combination of SM16 and Ad.E7) were harvested seven days after the second vaccination with Ad.E7 and subjected to FACS using MHC Class I tetramers loaded with the immunodominant HPV-E7 peptide. Panel A shows the average percentage of tetramer-positive $CD8^+$ T cells within the spleens (mean +/− SEM). * = $p<0.05$ compared to control. Panel B shows a representative FACS tracing from each group. The numbers in each box are the percentage of tetramer-positive, $CD8^+$ T cells.

Panels C: FACS staining of tumors. TC1 tumors from each treatment group were digested, and subjected to FACS two days after the second dose of Ad.E7, a time when the tumors in the combination group were rapidly shrinking, but still large enough to analyze. Panel C shows representative FACS tracings of side scatter versus CD8 expression. The number in each panel is the percentage of $CD8^+$ cells of the total tumor population (Figure 4, Panel F shows the averaged data from each group). In Panel D, cells from three tumors of each treatment group

were pooled, run through a Ficoll gradient, and subjected to FACS using MHC Class I tetramers loaded with the HPV-E7 peptide. The numbers in the upper boxes show the percentage of tetramer^{+} /CD8^{+} cells and the numbers in the lower boxes show the percentage of tetramer^{-}/CD8^{+} cells. This study was repeated with similar results.

Table 1

PCR and Protein Analysis of Tumor from Control and SM16-treated Tumors

Table 1A. Real-Time RT-PCR analysis of Tumors

Tumors (n=5 for each treatment group) from control and SM16-treated animals were treated for 5 days and then harvested, digested, and had RNA extracted. Equal amounts of RNA from each tumor in group were pooled and subjected to real time RT- PCR analysis (TC1, AB12, and LKR). RNA was normalized using β-actin levels. The fold change of each molecule, using the expression level in untreated controls as the denominator, was calculated. Each assay was run in at least quadruplicate.

		TC1		AB12		LKR	
	Primer	**Fold Change**	**p value**	**Fold Change**	**p value**	**Fold Change**	**p value**
Cytokines	**TNF-α**	3.7	0.0005	5.4	<0.001	2.1	0.008
	INF-γ	7.8	0.018	6.2	<0.001	1.4	0.03
	IL-12	1.5	NS	2.7	0.006.	21.2	<0.001
	IL-1*β*	2.0	0.001	3.3	<0.001	0.8	0.02
	IL-6	3.3	0.001	5.2	<0.001	0.4	<0.001
	IL-10	ND		9.7	<0.001	2.5	<0.001
	TGFβ			1.5	NS	1.0	NS
Chemokines	**Rantes**	1.1	NS	30.9	<0.001	2.2	0.008
	IP10	4.2	0.014	25.4	<0.001	2.5	<0.001
	MIG	4.5	0.0005	8.4	0.003	2.4	<0.001
	MCP-1	1.8	0.0005	2.4	<0.001	1.1	0.005
Other Mediators	**ICAM-1**	1.5	0.0018	2.6	0.07	1.5	0.02
	Arginase	0.2	0.01	0.9	NS	0.5	<0.001
	iNOS	3.1	0.04	5.4	<0.001	2.5	<0.001

Table 1B. Protein Measurements of AB12 Tissue Homogenates

Tumors (n=5 for each treatment group) from control and SM16-treated animals were treated for 5 days and then harvested, digested, and had protein extracted. Cytokine and chemokine levels for each tumor sample from each group were determined. Data is expressed as a ratio of SM16-treated to control levels. T-tests were used to compare groups.

Cytokine	**Fold change**	**P-value**
IL-6	2.72	0.01
INF-γ	1.35	0.1
TNF-α	0.84	0.64
IL-10	0.9	0.29
IL-12	0.87	0.57

Table 1B. Protein Measurements of AB12 Tissue Homogenates

Tumors (n=5 for each treatment group) from control and SM16-treated animals were treated for 5 days and then harvested, digested, and had protein extracted. Cytokine and chemokine levels for each tumor sample from each group were determined. Data is expressed as a ratio of SM16-treated to control levels. T-tests were used to compare groups.

Cytokine	Fold change	P-value
Chemokine		
Rantes	3.19	0.001
MIP-1a	2.46	0.02
MCP-1	1.75	0.04
IP-10	1.29	0.24